

# Millimeter-Wave GaN HEMT for Power Amplifier Applications

Kazukiyo JOSHIN<sup>†a)</sup>, Koza MAKIYAMA<sup>†</sup>, *Members*, Shiro OZAKI<sup>†</sup>, Toshihiro OHKI<sup>†</sup>, Naoya OKAMOTO<sup>†</sup>, Yoshitaka NIIDA<sup>†</sup>, *Nonmembers*, Masaru SATO<sup>†</sup>, *Member*, Satoshi MASUDA<sup>†</sup>, and Keiji WATANABE<sup>†</sup>, *Nonmembers*

**SUMMARY** Gallium nitride high electron mobility transistors (GaN HEMTs) were developed for millimeter-wave high power amplifier applications. The device with a gate length of 80 nm and an InAlN barrier layer exhibited high drain current of more than 1.2 A/mm and high breakdown voltage of 73 V. A cut-off frequency  $f_T$  of 113 GHz and maximum oscillation frequency  $f_{max}$  of 230 GHz were achieved. The output power density reached 1 W/mm with a linear gain of 6.4 dB at load-pull measurements at 90 GHz. And we extracted equivalent circuit model parameters of the millimeter-wave InAlN/GaN HEMT and showed that the model was useful in simulating the millimeter-wave power performance. Also, we report a preliminary constant bias stress test result.

**key words:** GaN HEMT, Millimeter-wave, Power amplifier, Device modeling

## 1. Introduction

With the spread of cellular and smart phones, higher capacity in mobile backhaul and wireless access networks would be required despite microwave frequency bands getting highly congested. It is becoming difficult to find available microwave frequency spectrum. Thus, millimeter-wave is expected to be an attractive frequency resource where wide bandwidth can be secured for high speed wireless communications. For example, the 70/80 GHz frequency band called E-band has attracted much attention as a multi-Gigabit capacity transport means in future networks due to its wide band spectrum of 5 GHz and a low cost of frequency licensing [1]. Some issues in promoting the millimeter-wave use are insufficient performance and high cost of the millimeter-wave devices. Especially, it is difficult to get a high output power amplifier with broad bandwidth.

GaN HEMT has attracted much attention as a device of millimeter-wave power amplifiers because of its several merits such as high breakdown voltage and high drain current due to high sheet carrier density of 2 dimensional electron gas (2DEG) of more than  $1 \times 10^{13} \text{cm}^{-2}$ . And AlGaIn/GaN HEMTs have been developed and used as microwave power amplifiers of cellular base stations due to their high output power and high efficiency performance [2].

Recently, device scaling of GaN HEMTs has been intensively pursued while focusing on their millimeter-wave operation and the gate electrode is expected to shrink to sub-0.1  $\mu\text{m}$  [3]–[7]. There are, however, some problems in

shrinking the device. One is a short-channel effect such as drain induced barrier lowering, low output resistance, and poor pinched-off characteristics. To suppress the short-channel effect, the barrier layer between the gate electrode and an electron transit channel should be thinned for shrinking the gate length. A thinner AlGaIn barrier layer, however, leads to lower 2DEG density and lower output power, and diminishes the merits of GaN HEMTs [8], [9]. Therefore, larger band gap materials with larger polarization effect such as InAlN have been considered for use as the barrier layer for millimeter-wave operations [10], [11]. InAlN/GaN HEMT has a twice higher 2DEG density than AlGaIn/GaN HEMT due to its larger conduction band discontinuity  $\Delta E_c$  and stronger spontaneous polarization effect [12], [13].

In a short-channel device, a buffer leakage current should also be considered to suppress the poor pinched-off characteristics. Thus, we studied a back barrier layer effect on InAlN/GaN HEMTs with an AlGaIn back barrier layer and an InGaIn back barrier layer [14]–[16] in conjunction with the charge trapping phenomenon. The polarization charges at upper and lower heterojunction interfaces of the InGaIn back barrier layer cause high electric field, confining 2DEG to the channel layer. The InGaIn back barrier layer suppresses the short-channel effect and enhances the output resistance.

The developed InAlN/GaN HEMT with a gate length of 80 nm exhibited a high drain current and high breakdown voltage of higher than 70 V. A cut-off frequency  $f_T$  of 113 GHz and maximum oscillation frequency  $f_{max}$  of 230 GHz were achieved.

In this paper, we describe the device structure and fabrication process of InAlN/GaN HEMTs and their DC and high frequency performance. Secondly, we explain an equivalent circuit model of InAlN/GaN HEMT, where we employ the Angelov GaN HEMT model. Its model parameters were extracted from the measured I-V and S-parameters, and the model simulation results were compared with power measurement results at 90 GHz. Finally, we report a preliminary constant bias stress test result.

## 2. InAlN/GaN HEMT Structure and Performance

### 2.1 Device Structure and Fabrication Process

Figure 1 shows our InAlN/GaN HEMT structure. Epitaxial layers of an InAlN barrier layer, an AlN spacer layer,

Manuscript received July 14, 2014.

<sup>†</sup>The authors are with Fujitsu Limited and Fujitsu Laboratories Ltd., 10-1 Morinosato-Wakamiya, Atsugi, 243-0197 Japan.

a) E-mail: joshin@jp.fujitsu.com

DOI: 10.1587/transele.E97.C.923

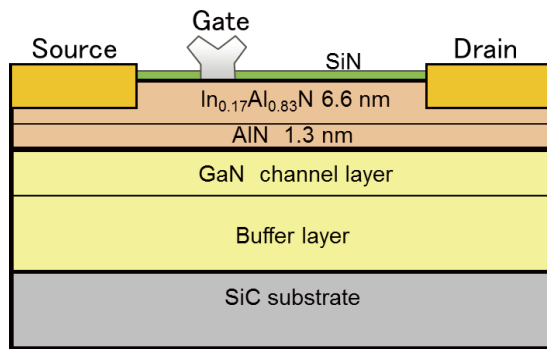


Fig. 1 InAlN/GaN HEMT structure with Y-shaped gate electrode.

a GaN channel layer, and a buffer layer were grown on a semi-insulated SiC substrate by the metal-organic chemical vapor deposition (MOCVD) technique. The Al mole fraction was 17% so that the lattice constant of the InAlN matched with GaN. The thickness was as less as 6.6 nm and the AlN was 1.3 nm. The device fabrication process was as follows. Firstly, the device isolation region was formed by ion-implantation. To achieve a millimeter-wave operation, source and drain ohmic electrodes must have a low contact resistance. Since a large band gap of InAlN makes it difficult to get a good ohmic contact, the InAlN layer was partially removed by dry-etching. Then, the ohmic metal layers were evaporated and annealed at 600°C. The ohmic contact resistance was around 0.8  $\Omega \cdot \text{mm}$ . A SiN dielectric film was deposited by plasma-enhanced chemical vapor deposition (PECVD). The gate footprints were defined by the electron-beam lithography and the SiN film was dry-etched. Gate metals of Ni/Au were evaporated and lifted-off. To reduce the gate resistance, a Y-shaped gate structure was formed using three photo resist layers. Fabricated GaN HEMTs have a gate width of  $2 \times 50 \mu\text{m}$ , a gate-source distance of 0.75  $\mu\text{m}$ , and a gate-drain distance  $L_{\text{gd}}$  of 2  $\mu\text{m}$ .

## 2.2 InGaN Back Barrier

To suppress the short-channel effect, we studied a thin GaN channel layer of 50 nm on the back barrier layer. Since the current collapse problem may occur due to electron traps in the barrier layer and the buffer layer just under the channel layer, we studied two kinds of barrier layers. One was an AlGaN barrier layer and the other was an InGaN barrier layer. Figure 2 shows the curve tracer  $I_{\text{D}}-V_{\text{D}}$  characteristics of fabricated InAlN/GaN HEMTs with an InGaN back barrier layer (right) and an AlGaN back barrier layer (left). Drain voltages were applied up to 10 V and 20 V to check the current collapse. The gate length was 0.12  $\mu\text{m}$ . The maximum gate voltage was 2 V by step of 0.5 V. The AlGaN back barrier HEMT caused a large current collapse as compared to the InGaN back barrier HEMT. We think that the electron traps in the AlGaN back layer or interfaces could have caused this current collapse.

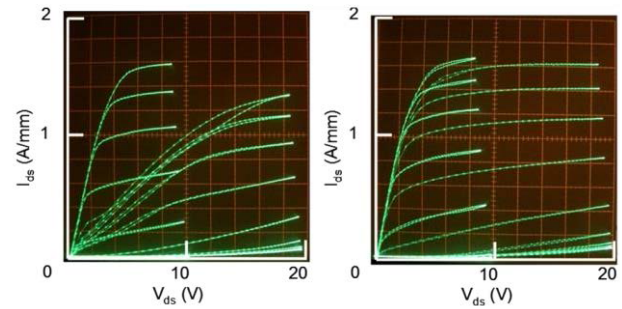


Fig. 2 Curve tracer  $I_{\text{D}}-V_{\text{D}}$  characteristics of InAlN/GaN HEMTs with an InGaN back barrier layer (right) and an AlGaN back barrier layer (left). Drain voltages were applied up to 10 V and 20 V to check the current collapse. Gate length is 0.12  $\mu\text{m}$ . GaN channel thickness is 50 nm.

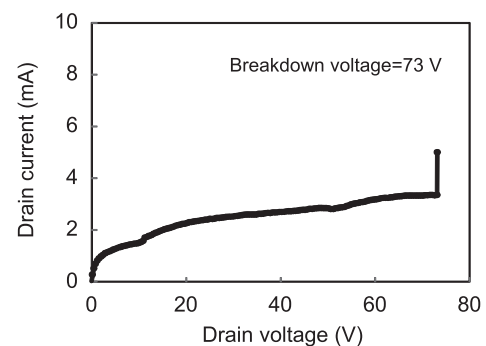


Fig. 3 Breakdown characteristics of 80 nm GaN HEMT.

## 2.3 DC Performance

The DC and RF performance of the fabricated InAlN/GaN HEMT was estimated with a semiconductor parameter analyzer and a vector-network analyzer. As shown in Fig. 2 of drain current-voltage characteristics, the maximum drain current was higher than 1.6 A/mm at  $V_{\text{GS}}$  of 2 V. There is a trade-off relationship between high frequency performance and breakdown voltage. A larger gate-drain distance  $L_{\text{gd}}$  leads to a higher breakdown voltage although the high frequency gain decreases. We optimized the  $L_{\text{gd}}$  to 2  $\mu\text{m}$  with a breakdown voltage of 73 V (Fig. 3).

## 2.4 High Frequency Performance

The high frequency performance of current gain cutoff frequency  $f_{\text{T}}$  and maximum oscillation frequency  $f_{\text{max}}$  was estimated by measured S-parameters. Figure 4 shows drain-source voltage dependence of  $f_{\text{T}}$  and  $f_{\text{max}}$ . It was observed that  $f_{\text{T}}$  was 113 GHz with  $f_{\text{max}}$  of 230 GHz at a drain voltage of 8 V.  $f_{\text{max}}$  enhanced as drain voltage increased due to a decrease of output capacitance and an increase of output resistance. At a drain voltage of 10 V,  $f_{\text{max}}$  reached 250 GHz. An  $f_{\text{T}}$  of more than 100 GHz was achieved at this drain voltage range and gate voltage of 0 V.

We estimated the millimeter-wave power performance of the fabricated GaN HEMT at 90 GHz with a load-pull measurement system of Focus Microwave Inc. and wafer

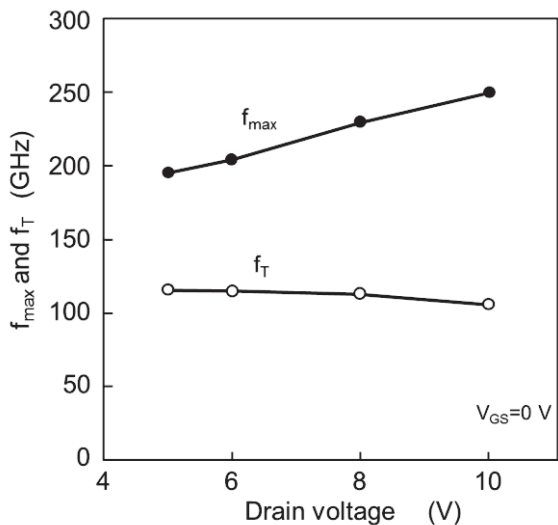


**Fig. 4** Drain-source voltage dependence of  $f_{max}$  and  $f_T$  estimated by S-parameters at  $V_{GS}$  of 0 V.

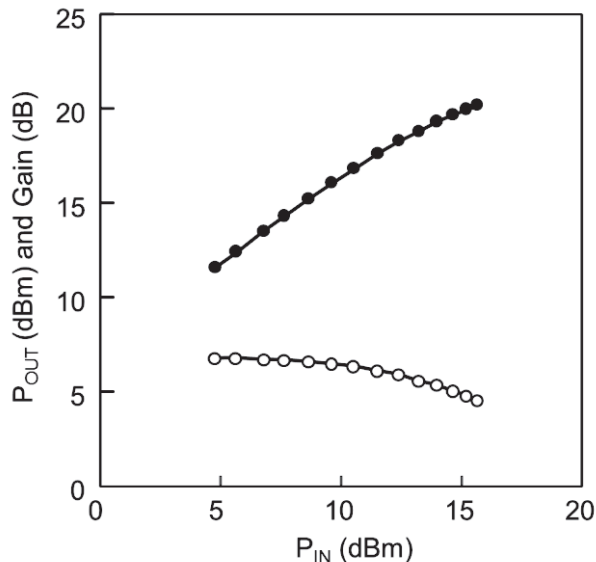


**Fig. 7** Pin-Pout characteristics of InAlN/GaN HEMT at 90 GHz and  $V_{DS}$  of 15 V and  $V_{GS}$  of  $-0.4$  V.

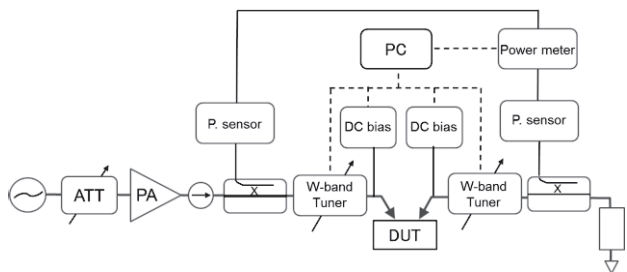


**Fig. 5** Load pull measurement set-up.

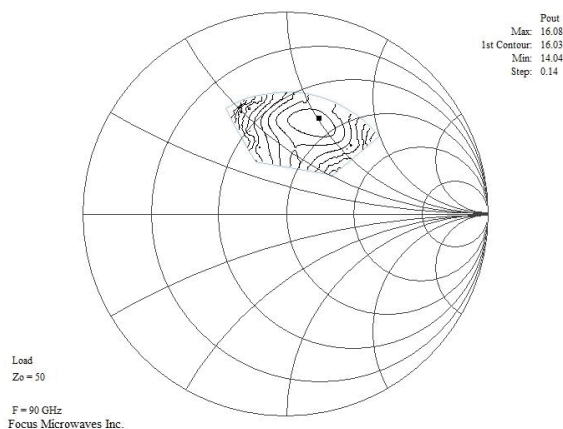


**Fig. 6** Load-pull measurement result at 90 GHz. The source tuner was tuned to give the maximum gain at a drain voltage of 15 V and gate voltage of  $-0.4$  V. The input power was 10 dBm. The contour step was 0.14 dB.

probe heads of GGB Industries Inc. The system used PC-controlled W-band auto-tuners (CCMT-WR10) as shown in Fig. 5. The input tuner was tuned to maximize the power gain. The input power was set to be constant at 10 dBm. The load-pull measurement result is shown in Fig. 6 at a drain voltage of 15 V and a gate voltage of  $-0.4$  V. The optimum load impedance was estimated to be  $31 \Omega + j 50 \Omega$  At

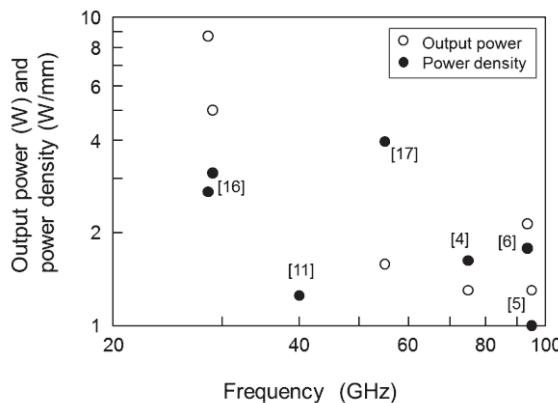


**Fig. 8** Reported millimeter-wave GaN HEMT power amplifier performance (○: output power, ●: output power density).

this matching condition, the input and output power performance was measured in Fig. 7. The linear gain was 6.8 dB and the maximum output power was 20.3 dBm where the input power was limited to 15.9 dBm due to a limitation of the drive power amplifier in our power measurement system. The fabricated GaN HEMT shows an output power density of more than 1 W/mm at a drain voltage of 15 V and at 90 GHz. Though the high output power density of 30 W/mm was reported at 4 GHz [18], it is limited to less than 2 W/mm in the W-band frequency range as shown in Fig. 8.

### 3. Equivalent Circuit Device Modeling

We extracted equivalent device model parameters from the measured DC  $I_D$ - $V_D$ , S-parameters, and load-pull measurement results of the millimeter-wave GaN HEMT. We employed the frequently-used Angelov model [19], which was commonly known as the GaN HEMT model. Figure 9 shows an equivalent circuit of the Angelov GaN HEMT model [20]. The drain current equations are expressed as

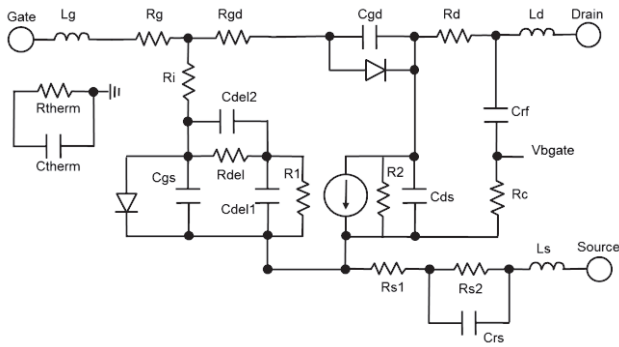


**Fig. 9** Equivalent circuit of the Angelov GaN HEMT model [20].

**Table 1** Extracted model parameters of 80 nm GaN HEMT with gate width of  $2 \times 50 \mu\text{m}$ .

$I_{pk}$	47.6 mA	$\lambda$	0.007
$V_{pks}$	0.1 V	$L_g$	30 pH
P1	1.24	$L_d$	30 pH
P2	0	$C_{gs}$	12 fF
P3	0.02	$C_{gs0}$	23 fF
$\alpha_r$	0.001	$R_g$	5 $\Omega$
$\alpha_s$	0.99	$R_d$	7 $\Omega$

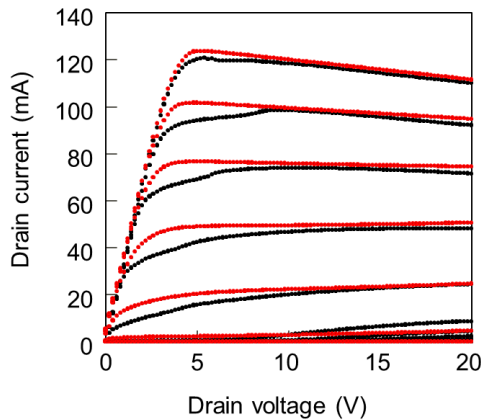


**Fig. 10**  $I_D$ - $V_D$  characteristics of measurement (black dots) and model simulation (red dots), ( $V_{GS} = -1.5 \text{ V}$  to  $1.5 \text{ V}$  by  $0.5 \text{ V}$  step).

follows.

$$I_{ds} = I_{pk}(1 + \tanh(\Psi_p)) \tanh(\alpha_p V_{ds})(1 + \lambda V_{ds}) \quad (1)$$

$$\Psi_p = \sinh(P_1((V_{gs} - V_{pk}) + P_2(V_{gs} - V_{pk})^2 + P_3(V_{gs} - V_{pk})^3)) \quad (2)$$

$$\alpha_p = \alpha_r + \alpha_s(1 + \tanh(\Psi_p)) \quad (3)$$

$$P_1 = g_{mpk}/I_{pk} \quad (4)$$

where  $V_{pk}$  and  $I_{pk}$  correspond to a gate voltage and a drain current at maximum transconductance  $g_{mpk}$ .  $\alpha_r$  and  $\alpha_s$  are saturation parameters. The functions of tanh and sinh will express the drain current and gm profile of GaN HEMTs. Table 1 shows the extracted model parameters of 80 nm GaN HEMT with a gate width of  $2 \times 50 \mu\text{m}$ . Figure 10 shows a comparison of the drain current-voltage characteristics between measurement and model simulation. A fairly good coincidence was observed except in the knee voltage

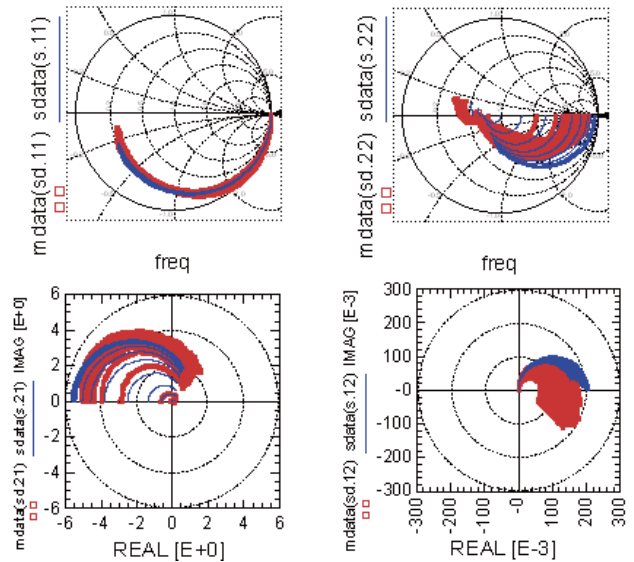


**Fig. 11** Measured (red lines) and modeled (blue lines) S-parameters from 0.1 GHz to 50 GHz at a drain voltage of 0 V to 20 V and gate voltage of 0 V.

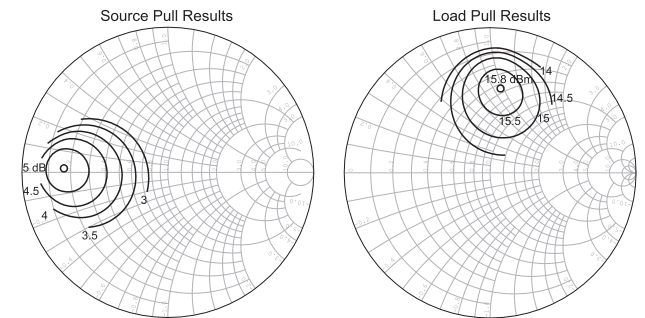


**Fig. 12** Load-pull simulation results with Angelov GaN model at 90 GHz and at a drain voltage of 15 V and gate voltage of  $-0.4 \text{ V}$ .

region where kinks were observed in the measured  $I_D$ - $V_D$  due to the charge trapping effect. As shown in Figure 11, the model parameters were extracted to fit the model simulation with the measured S-parameters, especially the reflection parameters of  $S_{11}$  and  $S_{22}$  which were important to design the input and output matching circuits of power amplifiers. It is difficult to get a good agreement between the measured and simulated S-parameters of  $S_{21}$  and  $S_{12}$ . Especially, there were phase differences in small  $S_{12}$  parameters.

Furthermore, to check the usability of the extracted Angelov GaN model parameters in millimeter-wave power amplifier design, load-pull simulation was done at 90 GHz (Fig. 12). The optimum load impedance was simulated to be  $28 \Omega + j 50 \Omega$  and agreed well with the load-pull measurement of  $31 \Omega + j 50 \Omega$  after an adjustment of the few extracted parameters. The Pin-Pout characteristics at 90 GHz were compared with the measurement results and Angelov GaN model simulation in Fig. 13. It can be seen that the model simulation results (lines) simulate the measurement results in a fairly good manner. So we assume that the Angelov GaN model parameters can be used in the design of

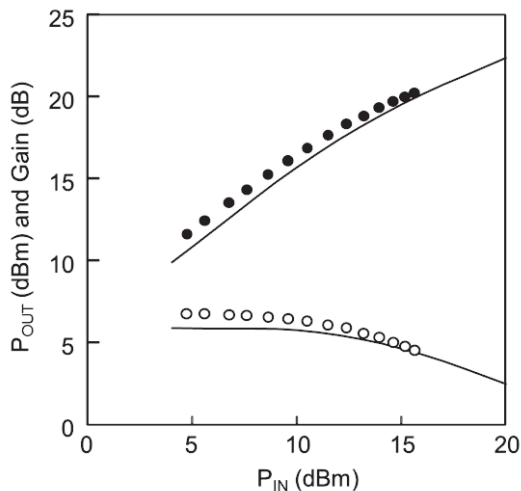


**Fig. 13** Modeled power characteristics at 90 GHz and at a drain voltage of 15 V and gate voltage of  $-0.4$  V. The modeled results (lines) simulate the measurement results (marks) in a fairly good manner.

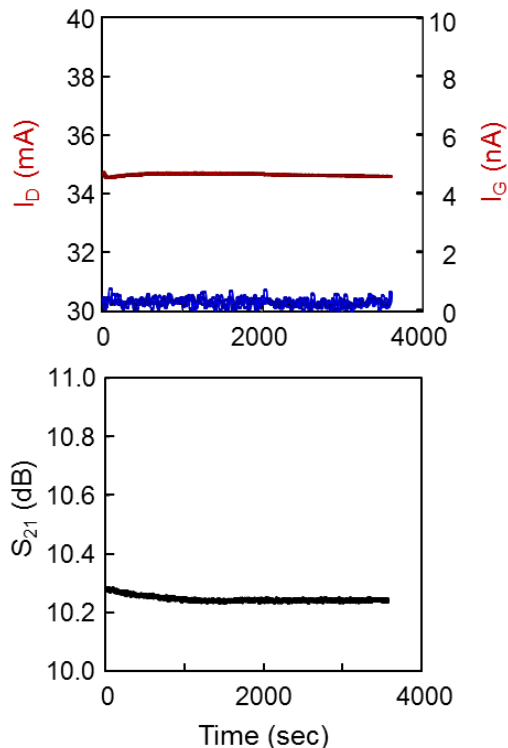


**Fig. 14** Preliminary constant bias stress test result of GaN HEMT at room temperature. The gate length was  $0.12 \mu\text{m}$  with a gate width of  $2 \times 50 \mu\text{m}$ . The drain voltage was 10 V and a gate voltage of  $-0.5$  V.  $S_{21}$  was measured at 1 GHz.

millimeter-wave power amplifiers.

#### 4. Bias Stress Test

The reliability of millimeter-wave GaN HEMTs has not been proved well. So we did a preliminary constant bias stress test as shown in Fig. 14. The gate length was  $0.12 \mu\text{m}$  with a gate width of  $2 \times 50 \mu\text{m}$ . The drain voltage was

10 V and a gate voltage of  $-0.5$  V.  $S_{21}$  was simultaneously measured at 1 GHz. Except for the initial time, there was no steep degradation in the drain current and  $S_{21}$ .

#### 5. Summary

We developed millimeter-wave GaN HEMTs for high power amplifier applications. The device with a gate length of 80 nm and an InAlN barrier layer exhibited high drain current and high breakdown voltage. A cut-off frequency  $f_T$  of 113 GHz and maximum oscillation frequency  $f_{max}$  of 230 GHz were achieved. The output power density reached 1 W/mm with a gain of 6.4 dB at load-pull measurements at 90 GHz. And, we extracted the equivalent circuit model parameters and showed that the model was useful in simulating millimeter-wave power performance of the InAlN/GaN HEMTs.

#### Acknowledgments

The research results have been achieved by “Agile Deployment Capability of Highly Resilient Optical and Radio Seamless Communication Systems,” the Commissioned Research of National Institute of Information and Communications Technology (NICT).

#### References

- [1] H. Hayashi, Y. Nakasha, M. Aota, and N. Sato, “Millimeter-wave impulse radio technology,” *FUJITSU Sci. Tech. J.*, vol.49, no.3, pp.350–355, 2013.
- [2] K. Joshin, T. Kikkawa, H. Hayashi, T. Maniwa, S. Yokokawa, M. Yokoyama, N. Adachi, and M. Takikawa, “A 174 W high-efficiency GaN HEMT power amplifier for W-CDMA base station applications,” *IEEE Int. Electron Device Meeting*, Washington D.C., pp.12.6.1–12.6.3, Dec. 2003.
- [3] T. Palacios, A. Chakraborty, S. Rajan, C. Poblenz, S. Keller, S. P. DenBaars, J. S. Speck, and U. K. Mishra, “High-power AlGaIn/GaN HEMTs for Ka-band applications,” *IEEE Electron. Device Lett.*, vol.26, no.11, pp.781–783, Nov. 2005.
- [4] Y. Nakasha, S. Masuda, K. Makiyama, T. Ohki, M. Kanamura, N. Okamoto, T. Tajima, T. Seino, H. Shigematsu, K. Imanishi, T. Kikkawa, K. Joshin, and N. Hara, “E-band 85-mW oscillator and 1.3-W amplifier IC’s using  $0.12\text{-}\mu\text{m}$  GaN MMICs for millimeter-wave transceivers,” *IEEE CSIC Symp. Dig.*, Monterey, CA, pp.199–202, Oct. 2010.
- [5] A. Brown, K. Brown, J. Chen, K. C. Hwang, N. Koliaas, and R. Scott, “W-Band GaN power amplifier MMICs,” *IEEE MTT-S Int. Microw. Symp. Dig.*, Baltimore, MD, June 2011.
- [6] M. Micovic, A. Kurdoghlian, A. Margomenos, D. F. Brown, K. Shinohara, S. Burnham, I. Milosavljevic, R. Bowen, A. J. Williams, P. Hashimoto, R. Grabar, C. Butler, A. Schmitz, P. J. Willadsen, and D. H. Chow, “92–96 GHz GaN power amplifiers,” *IEEE MTT-S Int. Microw. Symp. Dig.*, Montreal, QC, Canada, June 2012.
- [7] K. Shinohara, D. C. Regan, Y. Tang, A. L. Corrion, D. F. Brown, J. C. Wong, J. F. Robinson, H. H. Fung, A. Schmitz, T. C. Oh, S. J. Kim, P. S. Chen, R. G. Nagele, A. D. Margomenos, and M. Micovic, “Scaling of GaN HEMTs and schottky diodes for submillimeter-wave MMIC applications,” *IEEE Trans. Electron. Dev.*, vol.60, no.10, pp.2982–2996, Oct. 2013.
- [8] V. Tilak, B. Green, V. Kaper, H. Kim, T. Prunty, J. Smart, J. Shealy, and L. Eastman, “Influence of barrier thickness on the high-power performance of AlGaIn/GaN HEMTs,” *IEEE Electron. Device Lett.*,

- vol.22, no.11, pp.504–506, Nov. 2001.
- [9] M. Higashiwaki and T. Matsui, “Barrier thickness dependence of electrical properties and DC device characteristics of AlGaIn/GaN heterostructure field-effect transistors grown by plasma-assisted molecular-beam epitaxy,” *Jpn. J. Appl. Phys.*, vol.43, no.9A/B, pp.L1 147–L1 149, Aug. 2004.
- [10] Y. Yue, Z. Hu, J. Guo, B. Sensale-Rodriguez, G. Li, R. Wang, F. Faria, B. Song, X. Gao, S. Guo, T. Kosel, G. Snider, P. Fay, D. Jena, and H. G. Xing, “Ultrascaled InAlN/GaN high electron mobility transistors with cutoff frequency of 400 GHz,” *Jpn. J. Appl. Phys.*, vol.52, no.8S, pp.08JN14-1-2, May 2013.
- [11] B. P. Downey, D. J. Meyer, D. S. Katzer, J. A. Roussos, M. Pan, and X. Gao, “SiNx/InAlN/AlN/GaN MIS-HEMTs with 10.8 THz- $V$  Johnson figure of merit,” *IEEE Electron. Device Lett.*, vol.35, no.5, pp.527–529, May 2014.
- [12] J. Kuzmik, “Power electronics on InAlN/(In)GaN: Prospect for a record performance,” *IEEE Electron. Device Lett.*, vol.22, no.11, pp.510–512, Nov. 2001.
- [13] F. Medjdoub, M. Alomari, J.-F. Carlin, M. Gonschorek, E. Feltn, M. A. Py, N. Grandjean, and E. Kohn, “Barrier-layer scaling of InAlN/GaN HEMTs,” *IEEE Electron. Device Lett.*, vol.29, no.5, pp.422–425, May 2008.
- [14] T. Palacios, A. Chakraborty, S. Heikman, S. Keller, S. P. DenBaars, and U. K. Mishra, “AlGaIn/GaN high electron mobility transistors with InGaN back-barriers,” *IEEE Electron. Device Lett.*, vol.27, no.1, pp.13–15, 2006.
- [15] D. S. Lee, B. Lu, M. Azize, X. Gao, S. Guo, D. Kopp, P. Fay, and T. Palacios, “Impact of GaN channel scaling in InAlN/GaN HEMTs,” *IEEE Int. Electron. Device Meeting*, Washington, DC, pp.457–460, Dec. 2011.
- [16] C. F. Campbell, M. Y. Kao, and S. Nayak, “High efficiency Ka-band power amplifier MMICs fabricated with a 0.15  $\mu\text{m}$  GaN on SiC HEMT process,” *IEEE MTT-S Int. Microw. Symp. Dig.*, Montreal, QC, Canada, June 2012.
- [17] B. Heying, W. B. Luo, I. Smorchkova, S. Din, and M. Wojtowicz, “Reliable GaN HEMTs for high frequency applications,” *IEEE MTT-S Int. Microw. Symp. Dig.*, Anaheim, CA, pp.1218–1221, May 2010.
- [18] Y.-F. Wu, A. Saxler, M. Moore, R. P. Smith, S. T. Sheppard, P. M. Chavarkar, T. Wisleder, U. K. Mishra, and P. Parikh, “30-W/mm GaN HEMTs by field plate optimization,” *IEEE Electron. Device Lett.*, vol.25, no.3, pp.117–119, Mar. 2004.
- [19] I. Angelov, K. Andersson, D. Schreurs, D. Xiao, N. Rorsman, V. Desmaris, M. Sudow, and H. Zirath, “Large-signal modelling and comparison of AlGaIn/GaN HEMTs and SiC MESFETs,” *Proc. of Asia-Pacific Microwave Conf. Yokohama, Japan*, pp.279–282, Dec. 2006.
- [20] Verilog-A definition of Angelov GaN FET in Agilent Advanced Design System (ADS) 2012.08.



**Kazukiyo Joshin** received the B.S. degree in physics from Kyoto University in 1978, the M.S. degree in physics from the University of Tokyo in 1980, and the Ph.D. degree in electrical engineering from Osaka University in 1995. In 1980, he joined Fujitsu Laboratories Ltd., Kawasaki, where he worked on a research of low-noise HEMTs. He is currently engaged in research and development work on high-power and high-frequency GaN HEMTs at Fujitsu Laboratories Ltd., Atsugi. He received

the Ichimura Award for his work related to the development of low-noise HEMTs in 1989. He is a member of the IEICE and IEEE.



the Institute of Electronics, Information and Communication Engineers of Japan.

**Koza Makiyama** received the B.E. and M.E. degrees in electrical engineering from Osaka Institute of Technology, Osaka, Japan, in 1986 and 1988, respectively. In 1988, he joined Compound Semiconductor Laboratory in Fujitsu Laboratories, Ltd., Atsugi, Japan, where he has been engaged in research and development of HEMT technologies. He is currently engaged in research and work on millimeter-wave device. Mr. Makiyama is a member of the Institute of Electronics, Information and Communi-



**Shiro Ozaki** received the B.S. and M.S. degrees in applied chemistry from Yokohama National University, in 2002 and 2004, respectively. In 2004, he joined Fujitsu Laboratories Ltd., Atsugi, where he worked on a research of advanced materials for semiconductor devices. He is currently engaged in research and development work on process technology for GaN-HEMT. He received the best presentation award from the ISPlasma in 2013.

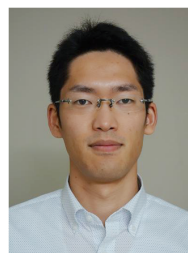


**Toshihiro Ohki** received the B.E. and M.E. degrees in Electrical Engineering from Waseda University, Tokyo, Japan, in 1999 and 2001, respectively. Since 2001, he has been with Fujitsu Laboratories Ltd., Atsugi, Japan, where he was engaged in the research and development of InP-based RTD/HEMTs and GaN-based HEMTs for high-speed optical and wireless communication systems. He is a member of the Japan Society of Applied Physics.

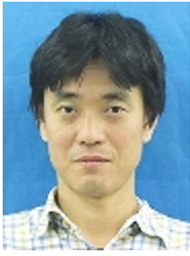


2002 through 2004. He is currently engaged in research and development of backside processing for GaN HEMT MMICs.

**Naoya Okamoto** received the B.E., M.E., and Ph.D. degrees from Osaka University, Osaka, Japan, in 1988, 1990, and 2001, respectively. In 1990, he joined Fujitsu Laboratories Ltd. and developed carbon-doped GaAs-based HBT grown by gas-source MBE. Afterwards, he studied GaAs surface passivation using gallium sulfide and developed InP-based HEMT and RTD/HEMT circuits. Also, he had been a researcher of Nanoelectronics Collaborative Research Center of The University of Tokyo from



**Yoshitaka Niida** received the B.S., M.S. and Ph.D. degree in physics from Tohoku University in 2005, 2009 and 2012, respectively. In 2012, he joined Fujitsu Laboratories Ltd., where he is currently engaged in research and development work on GaN HEMT high power amplifiers.



**Masaru Sato** received the B.E. and M.E degrees in electrical engineering from Tohoku University, Sendai, Japan, in 1996 and 1999, respectively. He joined Fujitsu Laboratories Ltd., Atsugi, Japan in 1999 and has been engaged in research on high-speed InP-based HEMT circuits for fiber-optic communication systems and millimeter-wave integrated circuits. His current research interests include development of microwave and millimeter wave MMICs. He is a member of the IEICE. He received the Young

Researcher's Award from the IEICE in 2006.



**Satoshi Masuda** received the B.E., M.E., and Ph.D. degrees in electrical engineering from Waseda University, Tokyo, Japan, in 1995, 1997, and 2009, respectively. In 1997, he joined Fujitsu Laboratories, Kanagawa, Japan, where he has been engaged in research and development of millimeter-wave monolithic ICs. His current research interests include modeling of active and passive components, millimeter-wave monolithic IC design, and flip-chip packaging. He received the Best Paper Award at the 2002

IEEE GaAs IC Symposium, the EuMC Microwave Prize at the 34th European Microwave Conference (EuMC 2004), and the Young Scientists' Prize by the Minister of Education, Culture, Sports, Science and Technology of Japan in 2006.



**Keiji Watanabe** received the B.E. and Ph.D. degrees in Tokyo University of Agriculture and Technology, Tokyo, Japan in 1986 and 2006. He joined Fujitsu Laboratories Ltd., Atsugi, Japan in 1986, where he has been engaged in research and development of materials for microelectronics.